Coincorporation of Nano-Silica and Nano-Calcium Carbonate in Polypropylene

Shilian Zhang,[1] Aiping Zhu,[1] Sheng Dai[2]

[1]*Department of Polymer Material and Engineering, College of Chemistry and Chemical Engineering, Yangzhou University, Yangzhou, 225002, People's Republic of China*
[2]*Department of Polymer Science, School of Chemical Engineering, The University of Adelaide, Adelaide, SA 5005, Australia*

Received 18 September 2010; accepted 7 December 2010
DOI 10.1002/app.33925
Published online 30 March 2011 in Wiley Online Library (wileyonlinelibrary.com).

ABSTRACT: In this study, various polypropylene (PP) nanocomposites were prepared by melt blending method. The effects of different spherical nanofillers, such as 50 nm $CaCO_3$ and 20 nm SiO_2, on the linear viscoelastic property, crystallization behavior, morphology and mechanical property of the resulting PP nanocomposites were examined. Rheological study indicated that coincorporation of nano-SiO_2 and nano-$CaCO_3$ favored the uniform dispersion of nanoparticles in the PP matrix. Differential scanning calorimeter (DSC) and polarizing optical microscopy (POM) studies revealed that the coincorporation of SiO_2 and $CaCO_3$ nanoparticles could effectively improve PP crystallizability, which gave rise to a lower supercooling temperature (ΔT), a shorter crystallization half-life ($t_{1/2}$) and a smaller spherulite size in comparison with those nanocomposites incorporating only one type of $CaCO_3$ or SiO_2 nanoparticles. The mechanical analysis results also showed that addition of two types of nanoparticles into PP matrix gave rise to enhanced performance than the nanocomposites containing $CaCO_3$ or SiO_2 individually.
 J Appl Polym Sci 121: 3007–3013, 2011

Key words: thermoplastic resin; microstructure; particle-reinforcement; rheological properties

INTRODUCTION

Isotactic polypropylene (*i*-PP) is one of the most important commercial thermoplastic materials because of its low cost and balanced properties, and has been found wide applications in food packaging, automotive industry, household appliances, and others. However, the small strength and toughness of *i*-PP limit its further applications. Therefore, the improvement in the strength and toughness of *i*-PP has received intensive attention from scientific researches to manufacturing industries. One effective approach is to prepare its nanocomposites by incorporating different nanoparticles to *i*-PP matrix. A remarkable improvement in the stiffness, toughness, and dimensional stability of *i*-PP can be achieved by introducing small amount of nanoparticles (1 wt % $\sim$ 10 wt %).[1] Among various *i*-PP nanocomposites, much attention has been paid to $CaCO_3$/*i*-PP composite systems, which reveals the enhanced mechanical property, low molding shrinkage and good processing property. Particle size, particle aspect ratio, particle size distribution, and the particle debonding before yielding are main parameters which affect the toughness of the $CaCO_3$/*i*-PP nanocomposites.[2] At a given particulate volume fraction, the composite strength increases with decreasing $CaCO_3$ size because smaller particles have higher surface area to weight ratios at a given particle loading.[3]

Conversely, SiO_2 nanoparticles are important nanoscale inorganic materials for reinforcing polymer properties.[4–8] For example, the tensile strength, yield strength, and yield strain of the P(VDF-TFE)/SiO_2 nanocomposites were substantially increased,[9] where P(VDF-TFE) is poly(vinylidene fluoride-*co*-tetrafluoroethylene). Nano-SiO_2 with different particle sizes has been used to prepare *i*-PP composites by Nitta et al.[10] They found that the addition of nano-SiO_2 caused a reduction in the average distance between adjacent particles. The linear growth rates became zero with the addition of 16 nm SiO_2. As a result, the mechanical properties of *i*-PP nanocomposites were significantly improved.[10]

The *i*-PP nanocomposites reinforced by incorporating $CaCO_3$ or SiO_2 nanoparticles have been well-

Correspondence to: A. Zhu (apzhu@yzu.edu.cn).
Contract grant sponsor: China Jiangsu Provincial Natural and Scientific Grant; contract grant number: SBK200930208.
Contract grant sponsor: China Jiangsu Provincial Innovative Grant; contract grant number: SBC200910282.
Contract grant sponsor: Jiangsu Province; contract grant number: 08KJA430003.

documented. To combine multiple natures of various nanoparticles in a polymer matrix, some researches reported the coincorporation of different types or shapes of nanoparticles into one polymer matrix. Yu et al. found that polyacrylonitrile/Na-montmorillonite/SiO_2 (PAN/Na-MMT/SiO_2) nanocomposites exhibited considerably enhanced moduli and thermal stability compared with PAN/Na-MMT and PAN/SiO_2 nanocomposites due to the synergistic reinforcing effect.[11] Coincorporation of nanoscale MMT and mesoporous MCM-41 (montmorillonite, with template) gave better toughness than the coincorporating of nano-SiO_2/OMMT (organic-montmorillonite) due to different interfacial structures between the fillers and the matrix.[12] Previous studies indicate that the synergistic effect of multiple inorganic particles can endow designed properties to a polymer matrix by selecting suitable (types, and sizes) nanofillers.

In the paper, nano-$CaCO_3$ with uniform size of 50 nm and nano-SiO_2 with uniform size of 20 nm were selected as the fillers to prepare *i*-PP nanocomposites via a melt compounding method. Rheology, topography, crystallization kinetics and mechanical property measurements were carried out to elucidate the coincorporation effect of spherical-shape nanofillers with different types and sizes. The results demonstrated that better flexural strength and notch impact strength are obtained for the *i*-PP composites coincorporating with both nano-SiO_2 and nano-$CaCO_3$ than those filling with single nano-$CaCO_3$ or nano-SiO_2. This significant synergistic reinforcing effect of nano-$CaCO_3$ and nano-SiO_2 was evident from rheology, topography, crystallization kinetics, and mechanical property studies.

EXPERIMENTAL

Materials

i-PP (F401) pellets were purchased from Yangzi Petrochemical Co. (China). Nano-SiO_2 (average diameter of 20 nm) and Nano-$CaCO_3$ (average diameter of 50 nm) were supplied by An Hui Jing Ye Nano Technology Co. (China). The dispersing agent (G4-1) was kindly supplied by Nanjing University of Technology (China).

Preparation of samples

Totally, 5.0 wt % additive concentrates were prepared by mixing nano-SiO_2 or nano-$CaCO_3$ with melted *i*-PP with the addition of G4-1 dispersing agent using a HAAKE Polylab Rheometer (Thermo Electron Co., USA). The *i*-PP nanocomposites were prepared by mixing different amounts of above additive concentrates and *i*-PP. In this study, five *i*-PP nanocomposites were prepared by filling nano-SiO_2 concentrate, nano-$CaCO_3$ concentrate or coincorporating nano-SiO_2 and nano-$CaCO_3$ concentrates (2% SiO_2/PP, 1.5%SiO_2/0.5%$CaCO_3$/PP, 1.0%SiO_2/1.0%$CaCO_3$/PP, 0.5%SiO_2/1.5%$CaCO_3$/PP, 2.0%$CaCO_3$/PP). The screw speed was fixed at 50 rpm, and the processing temperature and time was 180°C and 8 min. The resulting mixtures were hot-pressed under 14 MPa for 5 min at about 200°C into sheets of $\sim$ 1 mm thickness. Samples for mechanical properties test were prepared by melting previous compound mixtures for 10 min at 220°C and subsequent injection molding into rectangle shape specimens (12.8 $\times$ 1.28 $\times$ 0.30 cm^3) using a small injection molding machine (RR/TSMP2, Ray-Ran Test Equipment Co., England). All materials were dried at 75°C under vacuum for 8 h before property characterization.

TESTING AND CHARACTERIZATION

Rheological characterization

Rheological measurements were carried out on a rheometer (HAAKE RS600, Thermo Electron Co., USA) equipped with a 20 mm parallel plate geometry. The 1 mm thick *i*-PP nanocomposite samples were melted at 180°C for 5 min in the parallel plate fixture to eliminate residual thermal history, and then small amplitude oscillatory shear (SAOS) measurements were carried out in the frequency range between 0.01 and 100 s^{-1} immediately. The amplitude of deformation was set to 1%, which was within the linear elastic region as confirmed by an amplitude sweep with controlled shear deformation.

Morphology

The transmission electron micrographs (TEM) were taken from 80 to 100 nm thick, microtomed section using a Tecnai 12 transmission electron microscope (PHILIPS Co., Netherlands) at a 100 kV accelerating voltage.

Crystallization behavior

Crystallization of *i*-PP and its nanocomposites was studied using a 204 F1 differential scanning calorimeter (DSC, Netzsch Gerateban GmbH Instruments). In a typical DSC experiment, 5 $\pm$ 0.01 mg samples were used. The samples were initially melted at 200°C for 5 min to erase all previous thermal history. For nonisothermal crystallization, samples were cooled at 10°C/min. The crystallinity of the samples was determined from the heat of crystallization. Crystal morphology was studied using a polarizing optical microscope equipped with a hot-stage. The hot stage was held at a steady temperature with

± 0.2°C deviation by a proportional controller. The thin films of *i*-PP and its nanocomposites were sandwiched between a microscope slide and a cover glass, heated to 200°C and held at this temperature for 5 min, to allow the sample to melt completely and remove thermal memory. Cooling and heating rates used for dynamic experiments were 2°C/min and 10°C/min, respectively.

Mechanical testing

The flexural property was tested using a microcomputer control electronic universal testing machine (WDW-5, Shanghai Hualong Test Instruments Co., Ltd) at a speed of 2 mm/min. The testing samples had the dimension 12.8 × 1.28 × 0.30 cm^3. A pendulum impact device (TF2056, Jiangsu Mingzhu Testing Machine Co., Ltd) was used to determine notched impact strength at a rate of 3.5 m/s according to the standard GB/T 1843-2008, where 80 × 12.8 × 3 mm^3 samples with a style notch were used for the test.

RESULTS AND DISCUSSION

Linear viscoelastic properties

Rheological technique is always used to characterize the thermal–mechanical properties of polymer materials and to elucidate the structure–property relationship. For nanocomposites, the interaction between nanoparticles and polymer matrix could be studied by monitoring complex viscosity and other linear viscoelastic characteristics of nanocomposite melts as a function of frequency.[13–16] Figure 1(a,b) show the storage modulus (G') and complex viscosity (η*) dependence on dynamic oscillation frequency for *i*-PP (fill squares) and its nanocomposite. After incorporating 2.0 wt % nano-$CaCO_3$, the *i*-PP binary composite reveals significant drop in G′ and η* comparing with *i*-PP matrix, but only marginal decrease is evident for the binary nanocomposites prepared by filling 2.0 wt % of nano-SiO_2 into *i*-PP matrix. The significant reduction of G′ and η* is primarily attributed to the relatively large size of $CaCO_3$ nanoparticles, which causes *i*-PP chains to move easily in comparison with that filled with small size nano-SiO_2. On the other hand, the G′ and η* values of various SiO_2/$CaCO_3$/*i*-PP ternary nanocomposites (at fixed total filler concentration of 2.0 wt %) at low frequencies are between above two binary systems, but they are closed to the values of *i*-PP matrix. Most interestingly, the G' and η* values for the nanocomposites incorporating with 1.5% SiO_2/0.5% $CaCO_3$ and 0.5% SiO_2/1.5% $CaCO_3$ are identical within the experimental frequency region. Above results suggest that ternary nanocomposite systems should have

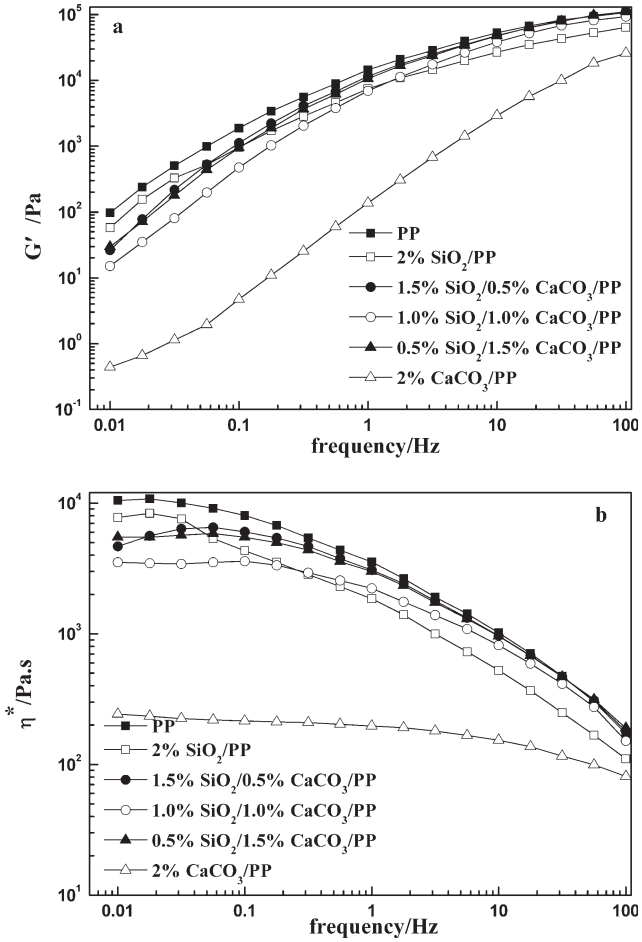

Figure 1 (a) Storage modulus G' and (b) complex viscosity η* as a function of oscillation frequency for i-PP and its nanocomposites.

different microstructures than binary systems, which affects the linear viscoelastic property of the resulting *i*-PP composite materials.

Linear viscoelastic characteristics derived from rheological measurements can be converted to a different representation using Cole-Cole plots for *i*-PP matrix and its nanocomposites (Fig. 2). The Cole–Cole plot can be used to sensitively report the formation of higher order structures in polymer melts.[13,14,17] In a typical Cole–Cole plot, the imaginary part of the viscosity is plotted against its real component.[14] The plot should be semispherical if higher order structures are absent and the melt relaxation behaviors could be described using a single Maxwell model with one relaxation time.[14,17] For many polymer blends, Cole–Cole plots yield two arcs, which are interpreted by the simultaneous occurrence of two processes with largely differing relaxation times.[18] Generally, for polymer composite melts containing inorganic fillers, the elastic component of the complex viscosity decreases and the polymer matrix always possesses a very short relaxation time. The Cole–Cole plot will display a

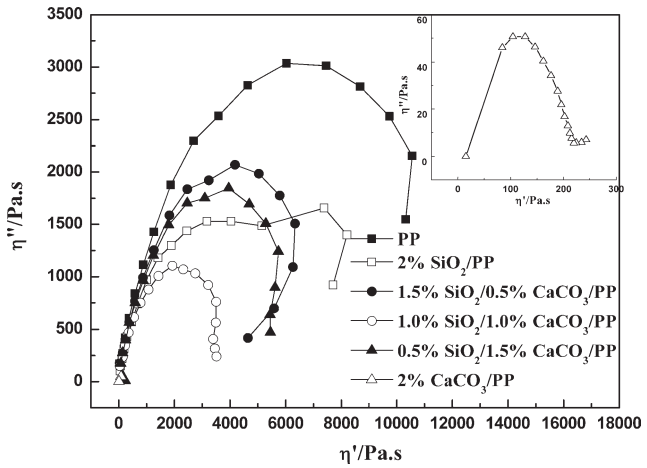

Figure 2 The Cole–Cole curves for i-PP and its nanocomposites. The upper right corner of the curve is for 2% CaCO3/PP.

tail or an increasing correlation if some microscale aggregation or network structure exists. From Figure 2, it can be found that the Cole–Cole plots of $SiO_2/CaCO_3/i$-PP ternary nanocomposites and *i*-PP matrix showed perfect arc-like curves, while the binary systems (SiO_2/i-PP and $CaCO_3/i$-PP) deviated significantly from single semispherical curves. These results suggested that some aggregates are formed within the binary nanocomposites, while the simultaneous coincorporation of nano-SiO_2 and nano-$CaCO_3$ favors the nanoparticle uniform dispersion in *i*-PP matrix. Such experimental results can be further reinforced by the morphological studies. The TEM images of the 0.5% SiO_2/1.5% $CaCO_3/i$-PP nanocomposite is shown in Figure 3

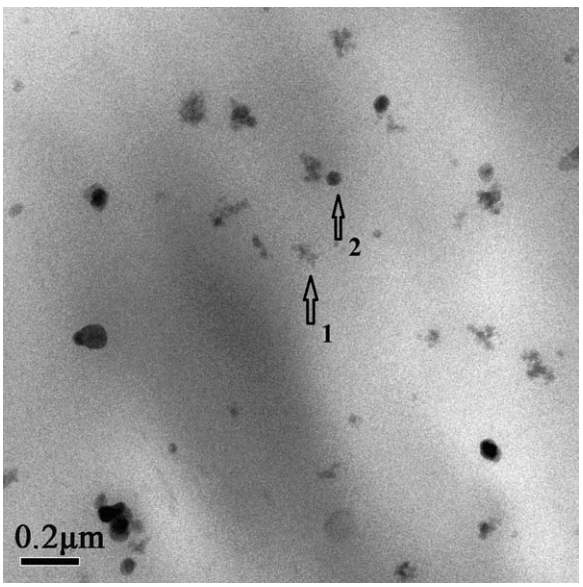

Figure 3 TEM image of the 0.5% SiO2/1.5% CaCO3/i-PP nanocomposite, where nano-SiO2 is indicated by 1 and nano-CaCO3 is indicated by 2.

and we are able to identify nano-SiO_2 and nano-$CaCO_3$ nanoparticle phases. Clearly, for the ternary system, both nanoparticles are randomly distributed in *i*-PP matrix.

Differential scanning calorimetry

Crystallization of polymer melts or melting of polymer crystals is accompanied significant heat release or absorption, which can be monitored by a differential scanning calorimeter (DSC).[19] The DSC thermograms of *i*-PP and its nanocomposites are shown in Figure 4, which are obtained from simple cooling-heating cycles. The thermodynamic parameters resulted from the DSC study are summarized in Table I. From Figure 4(a), we can find that the melting temperatures decrease slightly (about 2–3°C) with the addition of nanoparticles, while the enthalpies associated with the melting process (ΔH_m, normalized with respect to the mass fraction of *i*-PP in the composites) slightly increase in compared

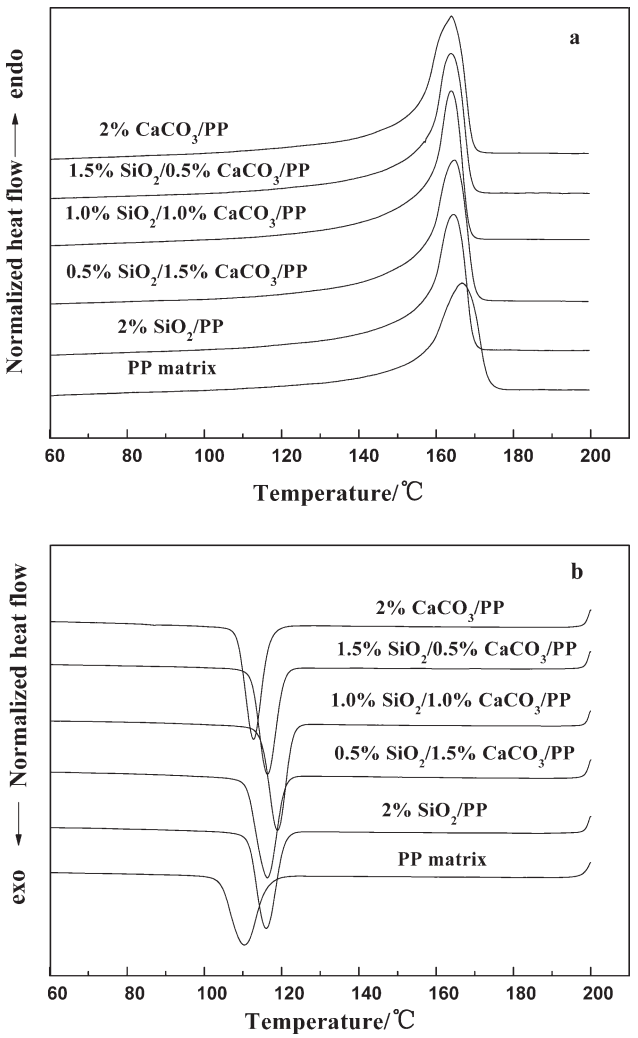

Figure 4 The DSC melting (a) and crystallization (b) curves of i-PP and its nanocomposite. The heating and cooling rates are 10°C/min.

TABLE I
Thermodynamic Parameters Associated with the Melting and Crystallization Processes of *i*-PP and Its Nanocomposites

	[a]T_c (°C)	[b] T_m (°C)	[c]ΔT (°C)	[d]ΔH_c (J/g)	[e]ΔH_m (J/g)	[f]X_c (%)	[g] $t_{1/2}$ (min)
i-PP matrix	110.3	166.7	56.4	−87.1	80.5	38.9	1.68
2.0% SiO_2/*i*-PP	116.0	164.5	48.5	−92.1	83.0	40.1	0.92
1.5% SiO_2/0.5% $CaCO_3$/*i*-PP	116.3	164.8	48.5	−99.4	84.4	40.8	0.98
1.0% SiO_2/1.0% $CaCO_3$/*i*-PP	118.9	164.0	45.1	−89.1	83.0	40.1	0.74
0.5% SiO_2/1.5% $CaCO_3$/*i*-PP	116.4	163.8	47.4	−88.1	83.3	40.3	0.91
2.0% $CaCO_3$/*i*-PP	112.7	163.9	51.2	−94.7	81.9	39.6	1.18

[a] T_c denotes the peak crystallization temperature.
[b] T_m denotes the peak melting temperature.
[c] $\Delta T = T_m - T_c$, denoting the supercooling temperature.
[d] ΔH_c denotes the crystallization enthalpy normalized with respect to the weight content of PP in the nanocomposites.
[e] ΔH_m denotes the melting enthalpy normalized with respect to the weight content of PP in the nanocomposites.
[f] X_c denotes the matrix crystallinity.
[g] $t_{1/2}$ denotes the crystallization half time.

with that of *i*-PP matrix. The results indicate that the melting process of *i*-PP is only slightly affected by filler incorporation, or the uploaded inorganic nanoparticles cannot seriously affect *i*-PP crystalline structure for either binary or ternary systems.

The degree of crystallinity can be approximately evaluated from the measured ΔH_m (J/g) according to following equation (after normalization for *i*-PP concentration):

$$X_c = \frac{\Delta H_m}{\Delta H_0}$$

where $\Delta H_0 \sim 207.1$ J/g is the melting enthalpy of 100% crystalline *i*-PP.[20] The introduction of nanoparticles lead to the slight decrease in T_m and the increase in X_c due to the nucleation effect of nanoparticles.[21] However, there is not obvious difference on the melting process of *i*-PP nanocomposites prepared by incorporating nano-SiO_2 or nano-$CaCO_3$.

Figure 4(b) shows the DSC nonisothermal crystallization behaviors of *i*-PP and its nanocomposites. Similar as melting process, the enthalpies associated with *i*-PP crystallization process slightly increase after incorporating inorganic nanoparticles. The crystallization temperature (T_c) of *i*-PP nanocomposites shifts to a higher temperature, while the supercooling temperature ($\Delta T = T_m - T_c$) decreases in comparison with that of *i*-PP matrix. For the binary nanocomposite systems, SiO_2/*i*-PP composite contains more particles and a lower ΔT comparing with those of $CaCO_3$/*i*-PP nanocomposite at fixed filler concentration of 2.0 wt %. For the ternary systems, ΔT further decreases as the coincorporated SiO_2 and $CaCO_3$ nanoparticles are uniformly distributed in *i*-PP matrix.

The relative crystallizability as a function of time for *i*-PP and its nanocomposites is shown in Figure 5. All curves display similar sigmoidal shapes. The curvature of the upper parts (near complete crystallization) in the plots is due to the spherulitic impingement in the later (growth) stages of crystallization.[22] From the curves, the half-life times ($t_{1/2}$) of nonisothermal crystallization were calculated and listed in Table I for a cooling rate of 10°C/min. It can be observed that *i*-PP filled with nanoparticles crystallizes faster than that of *i*-PP matrix. $t_{1/2}$ for the 1.0% SiO_2/1.0% $CaCO_3$/PP nanocomposite shows the lowest crystallization speed, which is nearly half of that of *i*-PP matrix. Previous DSC results indicate that the coincorporation of different spherical-shape nanofillers can effectively improve *i*-PP crystallizability.

Optical microscopy

Figure 6 shows the polarizing optical microscopic images of *i*-PP matrix and its nanocomposites filled with 2.0 wt % nanoparticles. The pure *i*-PP matrix shows typical spherulitic structure [Fig. 6(a)] with the largest size. After filling nanoparticles, the ultimate spherulitic size decreases. For the binary

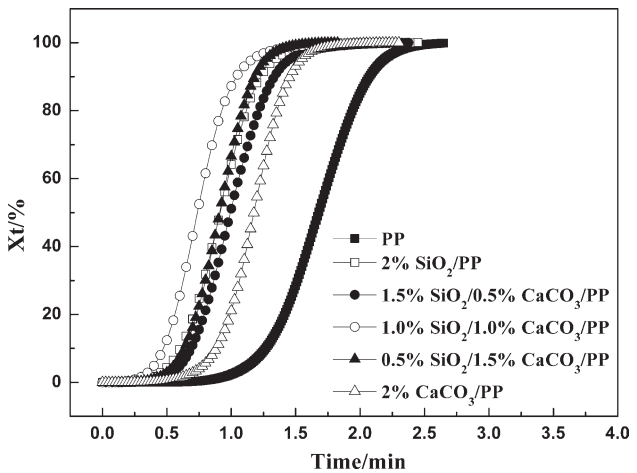

Figure 5 X_t versus time for i-PP and its nanocomposites.

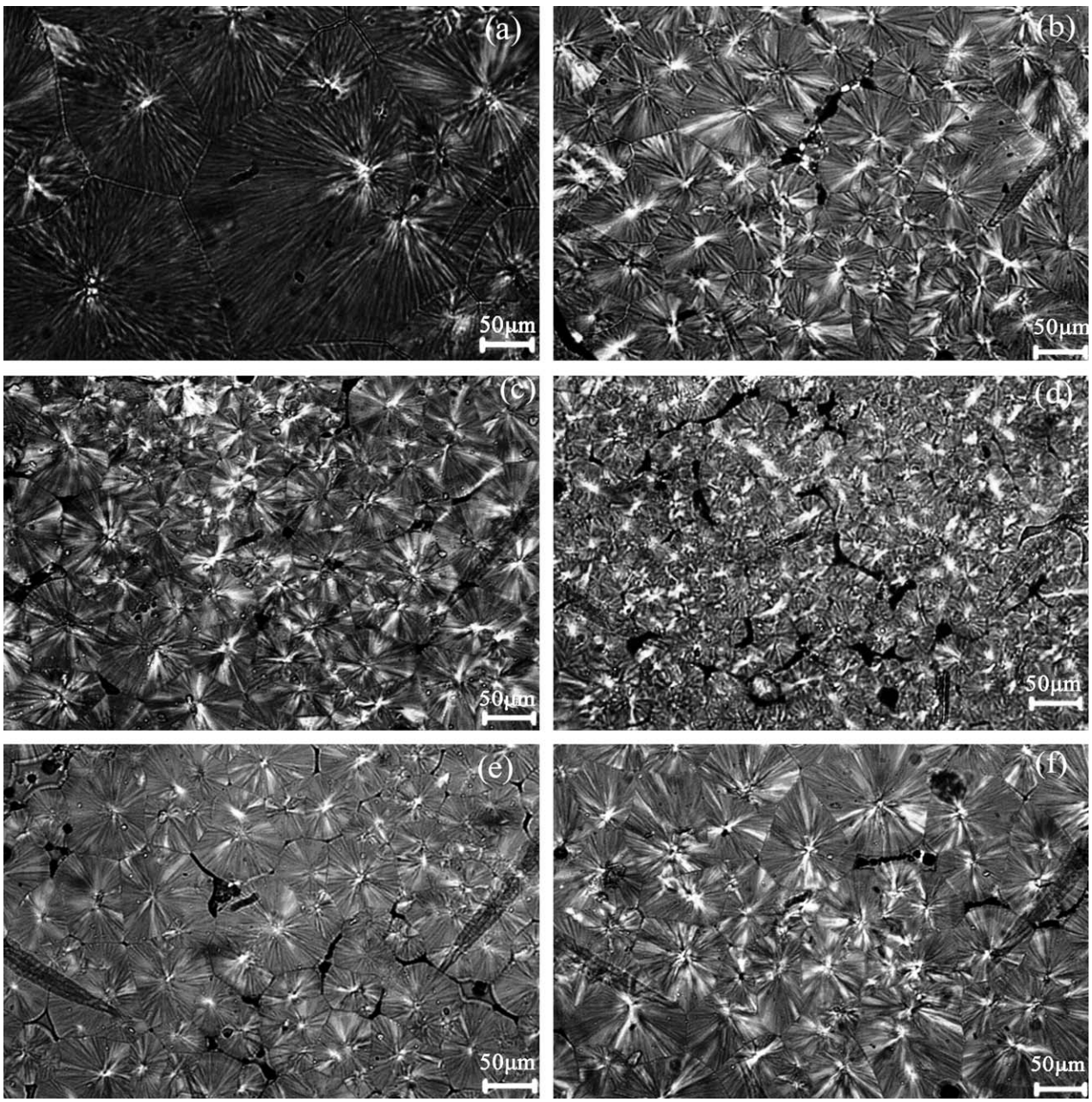

Figure 6 POM photographs of PP and its nanocomposites (a) PP, (b) 2% SiO_2/PP, (c) 1.5% SiO_2/0.5% $CaCO_3$/PP, (d) 1.0% SiO_2/1.0% $CaCO_3$/PP, (e) 0.5% SiO_2/1.5% $CaCO_3$/PP, and (f) 2% $CaCO_3$/PP.

nanocomposites prepared by incorporating one type of nanoparticles in Figure 6(b,f), the decrease in spherulite size is not significant. However, the ternary systems prepared by incorporating two types of nanoparticles display the remarkable reduction in the spherulites size of *i*-PP, especially for the *i*-PP nanocomposite containing nano-SiO_2 (1.0 wt %) and nano-$CaCO_3$ (1.0 wt%) [Fig. 6(d)]. This result indicates the best nucleation effect of 1.0% SiO_2/1.0% $CaCO_3$ in *i*-PP nanocomposite, which may be caused by the good dispersion of nanoparticles in *i*-PP matrix.

TABLE II
Flexural Strength and Notch Impact Strength of *i*-PP and Its Nanocomposite

Samples	Flexural strength (MPa)	Notch impact strength (kJ/m^2)
i-PP matrix	42.8 ± 1.8	3.5 ± 0.9
2.0% SiO_2/*i*-PP	47.2 ± 1.7	6.4 ± 0.5
1.5% SiO_2/0.5% $CaCO_3$/*i*-PP	53.5 ± 1.5	7.6 ± 0.6
1.0% SiO_2/1.0% $CaCO_3$/*i*-PP	55.7 ± 3.2	6.9 ± 0.8
0.5% SiO_2/1.5% $CaCO_3$/*i*-PP	51.5 ± 1.3	7.7 ± 0.3
2.0% $CaCO_3$/*i*-PP	45.9 ± 1.5	6.1 ± 1.1

Mechanical property

The mechanical properties of *i*-PP and its nanocomposites are compared in Table II. The mechanical properties of *i*-PP can be improved remarkably by the coincorporation of nanoparticles. At the same time, the ternary systems reveal better mechanical property than that of binary systems. For example, the flexural strength increases 13 MPa for the nanocomposite of 1.0 wt % SiO_2/1.0 wt % $CaCO_3$/*i*-PP, while the notch impact strength for the *i*-PP nanocomposites containing 0.5 wt % SiO_2 and 1.5 wt % $CaCO_3$ is approximately two times over that of *i*-PP matrix. Clearly, the *i*-PP nanocomposites prepared using two types of nanoparticles display noteworthy enhancement in the mechanical properties than those filled with one type of nanoparticles. The supposed reasons are considered to be, (1) coincorporation of different size of SiO_2 and $CaCO_3$ results in a uniform dispersion in matrix, and the stress can effectively transfer from the matrix to fillers. (2) superior crystallizability and smaller spherulitic size of SiO_2/$CaCO_3$/*i*-PP composite system.

CONCLUSIONS

Ternary nanocomposites have been prepared through coincorporation of spherical-shape nanofillers of nano-SiO_2 and nano-$CaCO_3$ into *i*-PP matrix via traditional melt compounding method. In comparison purpose, the binary nanocomposites of nano-SiO_2/*i*-PP and nano-$CaCO_3$/*i*-PP were also prepared at the same filler concentrations. The ternary system prepared by the coincorporation of SiO_2 and $CaCO_3$ nanoparticles results in a more uniform dispersion of nanoparticles in *i*-PP matrix. The crystallizability of *i*-PP is enhanced with the addition of SiO_2 and $CaCO_3$ nanoparticles, as evident by lower supercooling temperatures (ΔT), shorter crystallization half-life times ($t_{1/2}$) and smaller sizes of spherulites in comparison with the binary system filling only one type of $CaCO_3$ or SiO_2 nanoparticles. Resultantly, the SiO_2/$CaCO_3$/*i*-PP nanocomposites have superior mechanical properties comparing with the SiO_2/*i*-PP and $CaCO_3$/*i*-PP nanocomposites at the same filler loading.

References

1. Zhang, M. Q.; Rong M. Z.; Friedrich K. In Handbook of Organic-Inorganic Hybrid Materials and Nanocomposites, Vol. 2; Nalwa, H.S., Ed.; American Science Publishers: California, 2003.
2. Zuiderduin, W. C. J.; Westzaan, C.; Huétink, J.; Gaymans, R. J. Polymer 2003, 44, 261.
3. Fu, S. Y.; Feng, X. Q.; Lauke, B.; Mai, Y. W. Compos B 2008, 39, 933.
4. Douce, J.; Boilot, J. P.; Biteau, J.; Scodellaro, L.; Jimenez, A. Thin Solid Films 2004, 466, 114.
5. Reynaud, E.; Jouen, T.; Gauthier, C.; Vigier, G.; Varlet, J. Polymer 2001, 42, 8759.
6. Yang, H.; Zhang, X. Q.; Qu, C.; Li, B.; Zhang, L. J.; Zhang, Q.; Fu, Q. Polymer 2007, 48, 860.
7. Elias, L.; Fenouillot, F.; Majeste, J. C.; Cassagnau, P. Polymer 2007, 48, 6029.
8. Lin, J. C. Compos Struct 2008, 84, 125.
9. Cho, J. W.; Sul, K. I. Polymer 2001, 42, 727.
10. Nitta, K. H.; Asuka, K.; Liu, B. P.; Terano, M. Polymer 2006, 47, 6457.
11. Yu, T. S.; Lin, J. P.; Xu, J. F.; Chen, T.; Lin, S. L.; Tian, X. H. Compo Sci Technol 2007, 67, 3219.
12. Wang, N.; Fang, Q. H.; Shao, Y. W.; Zhang, J. Mater Sci Eng 2009, 512, 32.
13. Lertwimolnun, W.; Vergnes, B. Polymer 2005, 46, 3462.
14. Ábrányi, Á.; Százdi, L. B. P., Jr.; Vancsó, G. J.; Pukánszky, B. Macromol Rapid Commun 2006, 27, 132.
15. Galgali, G.; Ramesh, C.; Lele, A. Macromolecules 2001, 34, 852.
16. Ren, J. X.; Silva, A. S.; Krishnamoorti, R. Macromolecules 2000, 33, 3739.
17. Kiss, A.; Fekete, E.; Pukánszky, B. Compos Sci Technol 2007, 67, 1574.
18. Wu, D. F.; Zhang, Y. S.; Zhang, M.; Zhou, W. D. Eur Polym Mater 2008, 44, 2171.
19. Papageorgiou, G. Z.; Achilias, D. S.; Bikiaris, D. N.; Karayannidis, G. P. Thermochim Acta 2005, 427, 117.
20. Mark, J E. Polymer Date Handbook; Oxford University Press: New York, 1999.
21. Rybnikář, F. J Appl Polym Sci 1989, 38, 1479.
22. Jaina, S.; Goossensa, H.; Duinb, M. V.; Lemstra, P. Polymer 2005, 46, 8805.